JAAS Journal of Analytical Atomic Spectrometry

Inductively Coupled Nitrogen Plasma Mass Spectrometry Assisted by Adding Argon to the Outer Gas*

HIROSHI UCHIDA

Kanagawa Industrial Research Institute, 705–1, Shimoimaizumi, Ebina, Kanagawa 243–04, Japan

TETSUMASA ITO

Seiko Instruments Inc., 36–1, Takenoshita, Oyama-cho, Sunto-gun, Shizuoka 410–13, Japan

An inductively coupled nitrogen plasma (N_2 ICP) has been developed using a 40.68 MHz generator with a maximum rf power of 4 kW, and evaluated as an ion source for mass spectrometry (MS). The intermediate and central Ar flows are completely replaced with N_2; however, a certain amount of Ar should be added to the outer flow to maintain a stable plasma discharge. The sampling depth for the maximum analyte signals was found to be closer to the work coil, and the signal increases with the N_2 carrier flow rate up to 2.0 l min^{-1}. In the mass spectra obtained under the optimized conditions, N^+, O^+ and NO^+ are strongly observed, but the signal of Ar^+ is weak. The analytical sensitivity of the proposed N_2 ICP is almost equivalent to that of an Ar ICP for elements with low ionization potentials, but inferior for elements with high ionization potentials. The secondary discharge increases the average kinetic energy of the analyte ions, and its distribution in the N_2 ICP is wider than in the Ar ICP. A wide energy distribution also seems to lead to higher ratios of doubly charged and monoxide ions to singly charged ions. Space charge effects and ionization interference from co-existing elements are also discussed.

Keywords: *Inductively coupled nitrogen plasma; mass spectrometry; argon addition assistance; analytical characteristics; comparison with argon plasma*

The inductively coupled plasma (ICP) has been investigated as an ion source for mass spectrometry (MS) for the determination of ultratrace levels of elements.[1] The Ar ICP has been commonly used, because of its stable discharge at low radiofrequency (rf) power, high sensitivity and relative freedom from interferences. However, it is very difficult to avoid the mass spectral interferences resulting from plasma support Ar.[2] In particular, in the m/z range from 50 to 80, mass spectral overlapping between analytes and molecular ions caused by Ar (*e.g.*, ^{52}Cr and $^{40}Ar^{12}C$, ^{56}Fe and $^{40}Ar^{16}O$, and ^{80}Se and $^{40}Ar^{40}Ar$) is strongly observed. Further, the running costs for Ar consumption are a serious problem.

Mixed molecular gas ICPs have been investigated for the reduction of spectroscopic interferences[3–12] and other matrix effects.[6,7] Evans and Ebdon[3,4] discussed the effects of the addition of O_2 and N_2 to the central Ar flow on the reduction of polyatomic ion interferences. The addition of N_2 to the outer Ar gas was studied in an attempt to reduce oxide interference[5] and to eliminate the effects of co-existing Na[6] and K.[7] Lam and Horlick[8] also illustrated the effects of varying the sampler–skimmer spacing in a mixed ICP involving N_2 in the outer gas. Further, the addition of N_2 to the outer, intermediate and central Ar flows was investigated separately, mainly to reduce polyatomic interferences (ArCl, ArO, MO^+, *etc.*).[9–11] These mixed ICPs could tolerate a partial or total flow of N_2 in one of the three Ar flows of the original ICP. On the other hand, Louie and Soo[12] reported the addition of N_2 and H_2 to the main inlet for three types of Ar flow and discussed the analytical characteristics of the mixed ICPs. Tanaka *et al.*[13] reported N_2 and O_2 ICPs, where both the outer and central Ar flows were completely replaced with N_2 or O_2. However, neither of the replaced plasmas allowed the N_2 flow to be introduced into the intermediate gas. In addition, He–Ar or Xe–Ar mixed ICPs and several types of microwave-induced plasmas (MIPs) were investigated as the ion source for MS.[14]

No reports have been published on attempts to generate an N_2 ICP in MS. Two approaches to molecular gas ICPs have been applied in atomic emission spectrometry (AES): the first is a higher rf power and the second is a higher frequency (*e.g.*, 40.68 MHz).[15] Barnes and co-workers reported low power N_2[16,17] and CO_2[17] ICPs at 40.68 MHz and evaluated the light source for AES using a demountable torch with a special configuration.

In this study, attempts have been made to generate an N_2 ICP using an rf generator at 40.68 MHz with a maximum power of 4 kW,[18] and to evaluate the N_2 ICP as an ion source for MS. The structures of the coil, quartz torch and sampler were modified to achieve the replacement of Ar with N_2. Mass spectral profiles were obtained under the optimized plasma conditions, and the sensitivity was compared with that of an Ar ICP. Kinetic energy distribution, ratios of doubly charged and monoxide ions and matrix effects are also discussed.

EXPERIMENTAL

Instrumentation and Operating Conditions

The system used consisted of a quadrupole mass spectrometer (SPQ8000A, Seiko Instruments) and a specially ordered 40.68 MHz rf generator with a maximum power of 4 kW (Nippon Koshuha).[18] The structures of the work coil, quartz torch and sampler were improved in order to achieve a stable N_2 plasma discharge. A schematic diagram of the 3-turn work coil grounded at one end [16 mm long and 24.2 mm id without a Teflon (PFA) coating], the quartz torch modified from the demountable type for the low power N_2 and CO_2 ICPs in emission spectrometry[17] and the sampler (1.1 mm diameter orifice) with a thick top to prevent the damage caused by the secondary discharge is shown in Fig. 1. It should be noted that the gap between the outer and intermediate tubes was reduced to 0.5 mm in order to increase the swirl velocity of the outer gas flow, achieve a stable plasma discharge and keep the plasma away from the torch wall. A shielding system for the reduction of the plasma potential[19,20] could not be used, because the metal plate inserted between the quartz torch and

* Presented at the 1995 European Winter Conference on Plasma Spectrochemistry, Cambridge, UK, January 8–13, 1995.

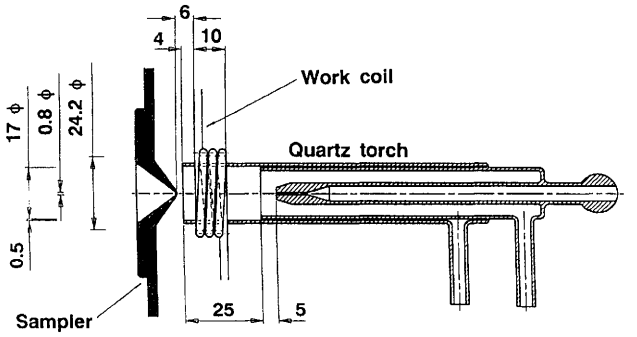

Fig. 1 Schematic diagram of the modified torch, work coil and sampler; dimensions in mm

the work coil melted at an rf power of more than 1.8 kW. In the outer, intermediate and central (carrier) gas flows, N_2 and Ar were introduced separately from each inlet. The chamber gas was introduced from an inlet attached to the spray chamber. Except for the above, the commercially available SPQ8000A ICP-MS system[18] was used without any modification for the N_2 ICP.

Final operating conditions for the proposed N_2 ICP are listed in Table 1. An Ar ICP was used as a starter for the N_2 ICP and also for the comparative study. The equipment used was the same as for the N_2 ICP, and the operating conditions are also given in Table 1. Details of the procedure for the conversion of the Ar ICP to the N_2 ICP and the optimization for the maximum analyte signals are discussed later.

Reagents

Stock solutions (10 ppm) of the analytes and the matrix for the investigation of co-existing interferences were prepared from commercially available 1000 ppm solutions for atomic absorption spectrometry (Wako Pure Chemicals or Kanto Chemicals). Working solutions were diluted before the measurements from the stocks using pure water from a Milli-Q system (Millipore) as a matrix of 3% ultrapure nitric acid (Tamapure-1000, Tamakagaku Kogyo). Ultrapure water (Tamakagaku Kogyo), where the concentration of trace impurities was less than 10 parts per 10^{12}, was used for the measurements of actual background ion counts.

RESULTS AND DISCUSSION

Nitrogen Plasma Discharge

The Ar ICP is required as a starter to generate the N_2 plasma discharge. After the ignition of the Ar ICP, the Ar flows were replaced with N_2 using the process shown in Table 2, which is similar to that of Yang *et al.*[17] The distance between the top of the quartz torch and the work coil was fixed at 4 mm. The introduction of N_2 into the intermediate gas was difficult below 4 mm, and a higher central flow rate of N_2 could not be achieved over 4 mm. A distance of 3–9 mm between the top of the work coil and the sampler is also recommended in order to facilitate the replacement of Ar with N_2.

Shrinkage of the plasma[6,10] and an increase in the reflected power were observed when N_2 was introduced into the outer gas, but the discharge could be maintained without any difficulty after rf matching. The addition of N_2 to the intermediate gas should be carried out slowly and carefully. By contrast, the replacement of Ar with N_2 in the central gas was easily achieved. The N_2–Ar mixed plasma spread out again, when the remainder of the Ar flow in the intermediate gas was replaced with N_2. A certain amount of Ar had to be used in the outer gas in order to achieve a stable plasma discharge. The stability of the proposed plasma discharge depended on this Ar flow rate and the concentricity of the three tubes in the modified quartz torch. For a torch with excellent concentricity, the flow rate of Ar could be reduced to 6, 4 and 1 l min^{-1} at rf powers of 2.5, 3.0 and 3.5 kW, respectively. A high flow rate of Ar (low flow of the added molecular gas) in any of the three tubes seems to contribute to the stable discharge of the mixed ICPs.[8–13]

On the other hand, Yang *et al.*[17] reported a complete N_2 plasma at 2.2 kW using a 40.68 MHz rf generator in AES; however, small amounts of Ar should be added to the outer gas in the proposed MS system. One of the differences between AES and MS systems is the presence of the sampler in front of the gas outlet of the quartz torch, shown in Fig. 1, which might affect the gas flows in the N_2 ICP. Since the concentricity of the quartz torch is a major requirement, the gas flow might be one of the important factors for the stability of the plasma discharge. A flow of 10 l min^{-1} of Ar was added to the outer gas in the latter experiments.

A bright discharge with a ring structure was clearly observed around the top of the sampler, and the signals of $^{63}Cu^+$ and $^{65}Cu^+$ were easily detected in the MS spectra (shown later in Fig. 5). These phenomena are probably caused by a secondary discharge, which cannot be removed without employing a shielding system in the present mass spectrometer, which has a work coil grounded at one end.

Table 1 Operating conditions for the N_2 and Ar ICPs*

	N_2 ICP	Ar ICP
Forward power/kW	2.5	1.0
Outer gas flow rate/l min^{-1}	N_2 20.0 Ar 10.0	Ar 16.0
Intermediate gas flow rate/l min^{-1}	N_2 1.0	Ar 1.0
Carrier gas flow rate/l min^{-1}	N_2 1.6	Ar 0.65
Sampling depth/mm above the work coil	6	13

* The same modified torch was used in both ICPs.

Distribution of Analyte Ions Along the Plasma Axis

The spatial distribution of analyte ion signals along the axis of the N_2 ICP was investigated first. The discharge could be maintained when the plasma was approaching the sampler, even if the reflected power was increased for an instant. However, it disappeared when the plasma was taken away from the sampler. In the distribution measurement, the replacement of Ar with N_2 was carried out at a sampling depth of 9 mm above the work coil, and the plasma was then moved to the sampler.

The results obtained for the distribution are shown in Fig. 2. The sampling depth for the maximum analyte signal was found to be approximately 13 mm from the top of the work coil in the Ar ICP, which is common for many elements.[18] However, the maximum signals were observed at 6 mm for Co^+ and Y^+, and at 3 mm for Pb^+. The reason for the different behaviour of Pb^+ is not known. The signals were decreased considerably at >9 mm above the work coil, which might be caused by shrinkage of the plasma. Even if the plasma spreads in the final replacement of Ar with N_2, the outer part of the plasma might be cooled by molecular N_2. The decrease in the sensitivity in the outer part of the plasma is consistent with the results obtained from the Ar–molecular gas mixed ICP,[5,6,9,10,12] where the lower position was recommended as the sampling depth, compared with the Ar ICP. A sampling position of 6 mm was used subsequently.

Table 2 Procedure for conversion of the Ar ICP to the N_2 ICP

Step	Sampling depth/ mm	Rf power/ kW	Outer gas flow rate/l min^{-1}		Intermediate gas flow rate/l min^{-1}		Central gas flow rate/l min^{-1}	
			Ar	N_2	Ar	N_2	Ar	N_2
1	15	1.0	16		1.0		0.65	
2	6							
3			20					
4		2.0						
5			15	15				
6					0.75	0.75		
7		2.5						
8							0	0.6
9					0	1.0		
10			10	20				
11								1.6
Final	6	2.5	10	20		1.0		1.6

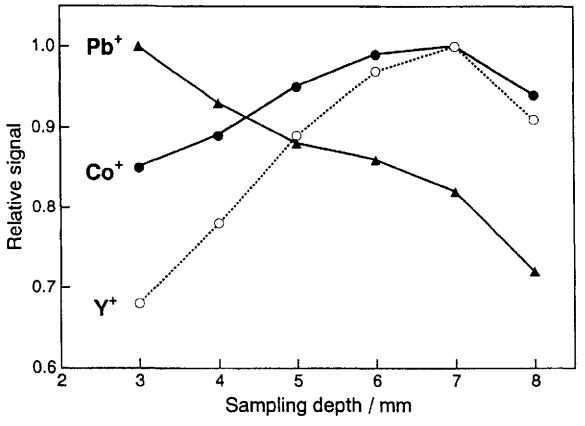

Fig. 2 Distributions of the relative analyte ion signals along the axis; N_2 carrier flow rate, 1.6 l min^{-1}

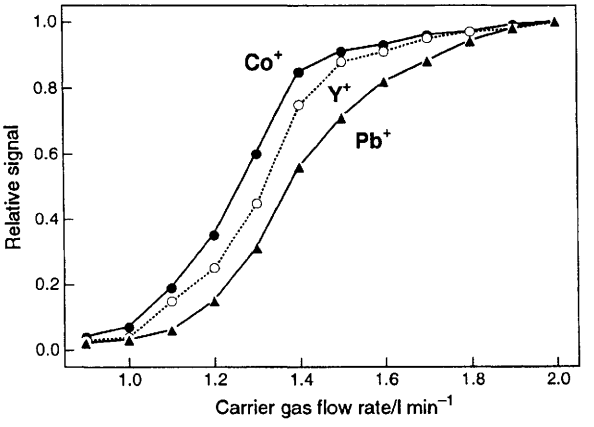

Fig. 3 Effect of the N_2 carrier flow rate on the relative ion signals; sampling depth, 6 mm above the work coil

Effect of the Central Gas Flow Rate on the Analyte Ion Signal

The carrier gas flow rate is one of the most significant factors affecting the analytical characteristics of the ICP, *e.g.*, sensitivity, and chemical and ionization interferences. In the Ar ICP, the maximum signals were found at flow rates from 0.5 to 1.0 l min^{-1} in both AES and MS. The rate of introduction of the analyte into the plasma increases with the carrier flow rate; however, the analyte cannot acquire sufficient energy for excitation or ionization at higher flow rates. Maximum signals were obtained at 0.65 l min^{-1} in the Ar ICP-MS system used, which is slightly lower than in the 27.12 MHz ICP-MS system.[18]

Fig. 3 indicates the effect of N_2 carrier flow rate on the ion signals for Co^+, Y^+ and Pb^+. Analyte signals for all the ions increase up to an N_2 flow rate of 2.0 l min^{-1}. Some blank signals for Y^+ and Ba^+ were found at flow rates below 1.0 l min^{-1}; these might be from the quartz torch. The plasma might hit the quartz wall; however, it was not possible to confirm this. These blank signals decreased with an increase in the N_2 carrier flow rate. The sensitivity appears to increase 10-fold at flow rates >1.6 l min^{-1} compared with that at a flow rate of 1.0 l min^{-1}. There might be significant differences in the analytical characteristics of N_2 and Ar ICPs.

The effect of the central gas flow rate was examined further in order to clarify the N_2 ICP characteristics. A chamber gas is sometimes used for the reduction of ArO^+ interference with use of a shielding system,[20] and it does not affect the rate of introduction of the analytes into the plasma. The results obtained are shown in Fig. 4. The relative signals in Fig. 4 were calculated by assuming that the signal obtained at an N_2 carrier flow rate of 1.0 l min^{-1} without chamber gas is 1.0. The

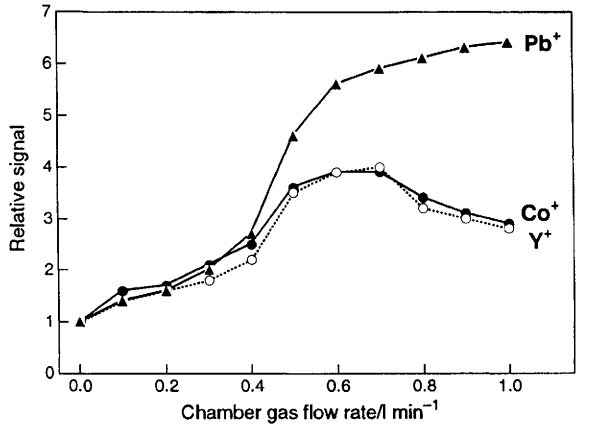

Fig. 4 Effect of the chamber N_2 flow rate on the relative ion signals; sampling depth, 6 mm above the work coil and N_2 carrier flow rate, 1.0 l min^{-1}

calculated relative signals increase with the chamber gas flow rate up to 0.7 l min^{-1} for Co^+ and Y^+, and up to 1.0 l min^{-1} for Pb^+, even if the rate of introduction into the plasma is kept constant. The signals of Pb^+ also exhibit a slightly anomalous behaviour, as shown by the signal distributions along the plasma axis.

In the light of the results obtained from analyte ion signal distributions, the hot region available for the ion source in the proposed N_2 ICP exists in the deeper part of the plasma, and is pushed out to the sampling position at higher central gas flow rates. Further, the sampling position for the maximum

analyte signals should be closer to the work coil, compared with that in the Ar ICP. An N_2 carrier flow rate of 1.6 l min^{-1} without a chamber gas flow was used at a sampling depth of 6 mm in the latter.

Nitrogen ICP Mass Spectra

Mass spectra of the proposed N_2 ICP, obtained under the optimized analytical conditions, are shown in Fig. 5 over the m/z range from 5 to 70. Fig. 5(*a*) and (*b*) were obtained by ultrapure water nebulization with low sensitivity. Signals for N^+, O^+ and NO^+ are strongly observed, and O^+ seems to be caused by the introduced water. The signal ratio of N_2^+ to N^+ is lower than that of the N_2-MIP,[21] and the concentration of molecular nitrogen (N_2) seems to be less than 1% of the nitrogen atoms (N) in the optimized region. Further, the Ar added to the outer gas does not seem to contribute to the ionization of the analyte, because the Ar^+ signal indicated in Fig. 5(*b*) is very weak and remains constant, even if the added Ar flow rate increases from 6 to 15 l min^{-1}. The proposed plasma might be termed an N_2–Ar mixed ICP as regards total gas composition, but the mass spectra indicate that the optimized region is actually an N_2 plasma. The term 'Ar-assisted N_2 ICP' might be appropriate for the proposed plasma.

On the other hand, Fig. 5(*c*) was obtained from a 3% nitric acid solution with relatively high sensitivity, where the detector was masked in the m/z range from 14 to 17 and from 29 to 31 in order to avoid damaging the detector. The concentration of the analytes was 100 ppb. Signals for $^{63}Cu^+$ and $^{65}Cu^+$ are readily observed; these are caused by the secondary discharge. Mass spectral interferences resulting from Ar seem to be less pronounced than those in the Ar ICP.

Sensitivity and Detection Limit

A comparison of the sensitivities and detection limits of the N_2 and Ar ICPs was carried out. The results obtained are summarized in Table 3. The signals in both ICPs were measured under the same operating conditions and with the same mass spectrometer. The sensitivity is indicated as counts per second per ppb, and the detection limit as the concentration corresponding to a signal-to-background noise ratio of three. Ultrapure water was used for the measurement of the actual background signal for each element.

The sensitivity seems to depend on the first ionization potential (IP), and to be equal to that in the Ar ICP for elements with low IPs (Sr^+, Y^+, Ba^+ and La^+). However, the signals per ppb for other elements, particularly those with high IP values, are smaller. Further, the sensitivity for heavy ions (over m/z 200) is lower, even if their IP values are also low. The calculated values of the detection limit follow the same trend as for the sensitivity, except for Ti^+, V^+ and Zn^+, where the background signals are smaller in the N_2 ICP than those in the Ar ICP.

The detection limit for $^{56}Fe^+$ is improved by more than 1000 times in the proposed N_2 ICP, because the detection at m/z 56 is interfered with by ArO^+ in the Ar ICP. The actual detection power is increased 10-fold compared with that of the Ar ICP, even taking the detection of $^{57}Fe^+$ into account in both ICPs. The detection limit for $^{80}Se^+$ is also improved, since the signal counts of Ar_2^+ decrease considerably. However, the actual detection power is almost equivalent to that of the Ar ICP, because of the high IP of Se and the abundance of ^{78}Se (23.8%). An improvement in ^{75}As detection might be expected by the reduction of $ArCl^+$ in hydrochloric acid nebulization.

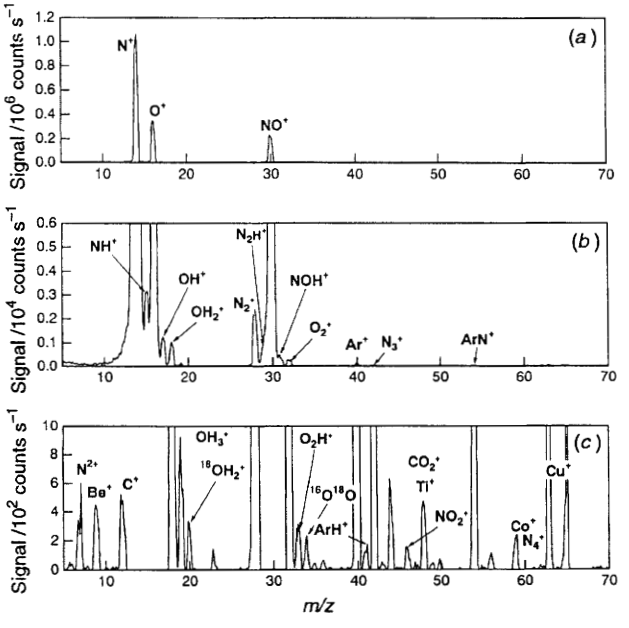

Fig. 5 Mass spectra of the N_2 ICP under optimized conditions: (*a*) and (*b*) obtained under low sensitivity conditions; (*c*) obtained under high sensitivity conditions with masked detector in the m/z ranges from 14 to 17 and from 29 to 31

Kinetic Energy Distribution of the Analyte Ions

The ion kinetic energy measurements are also interesting with respect to the ICP-MS characteristics.[22,23] As the ion lens system in the mass spectrometer used does not act as an energy filter, the ion kinetic energy can be discussed by use of the retarding dc quadrupole rod bias. Plots of ion counts *versus* the retarding voltage were obtained for Co^+ and Pb^+ in the N_2 and Ar ICPs, and the normalized results are shown in Fig. 6. The average energy values, obtained at a relative signal of 0.5, were found to be approximately 28 (Co^+) and 29 eV (Pb^+) in the Ar ICP, and 31 (Co^+) and 36 eV (Pb^+) in the N_2 ICP.

These values are higher than those obtained with a 40.68 MHz Ar ICP with a shielding system,[18] where the value obtained for the average energy was approximately 6 eV. The increase in this average value seems to depend on the secondary discharge. The average energy value in the N_2 ICP is slightly higher than that in the Ar ICP. Further, the width of the energy distribution for each ion is calculated as the difference between the two retarding voltage values, obtained at relative signals of 1.0 and 0. The width of the energy distribution was found to be larger in the N_2 ICP than in the Ar ICP, as shown in Fig. 6.

Ratios of Doubly Charged and Monoxide Ions

Doubly charged and monoxide ions of analytes frequently interfere in ultratrace determinations by ICP-MS; however, their concentrations in the ICP also yield interesting information with respect to analytical characteristics. Ratios of doubly charged and monoxide ions to singly charged analyte ions are summarized together with the first and second IP values in Table 4. The ratio of doubly to singly charged ions is lower in the N_2 ICP than in the Ar ICP for Y^+, Ba^+ and Ce^+, whose second IP values are relatively low. In contrast, the ratio is higher for Mo^+ and Pb^+, whose second IP values are higher. As shown in Fig. 6, the kinetic energy distribution in the N_2 ICP is wider than in the Ar ICP. A high ratio of doubly charged ions might be linked to a high concentration of higher energy ion species.

The ratio of monoxide ions to singly charged ions was found to be higher in the N_2 ICP; this might be caused by the

Table 3 Comparison of the sensitivities and detection limits of the N_2 and Ar ICPs

				Sensitivity			Detection limit		
Element	*m/z*	Abundance (%)	IP eV	N_2 ICP/ counts per ppb	Ar ICP/ counts per ppb	Ratio (N_2:Ar)	N_2 ICP (ppt)*	Ar ICP (ppt)*	Ratio (N_2:Ar)
Be	9	100	9.32	1200	9400	0.13	30	2	15
Ti	48	73.8	6.82	2300	2300	1.0	0.9	2	0.45
V	51	99.8	6.74	2300	2900	0.79	0.5	4	0.13
Cr	52	83.8	6.76	4400	5700	0.77	4	4	1.0
Mn	55	100	7.43	1900	3300	0.58	50	0.8	63
Fe	56	91.7	7.86	1400	2400	0.58	1	700	0.0014
	57	5.8		38	65	0.58	15	10	1.5
Co	59	100	7.86	1700	3500	0.49	0.7	0.5	1.4
Zn	66	27.9	9.39	330	470	0.70	4	5	0.8
Ga	69	60.1	6.00	1100	2000	0.55	8	2	4.0
As	75	100	9.81	120	280	0.43	0.5	0.2	2.5
Se	78	23.8	9.75	28	70	0.40	30	10	3.0
	80	49.6		74	190	0.39	15	3000	0.005
Sr	88	87.9	5.69	2600	2300	1.1	5	2	2.5
Y	89	100	6.38	3100	2900	1.1	0.2	0.08	2.5
Mo	98	24.1	7.10	530	800	0.66	4	1	4.0
Ag	107	51.8	7.57	690	1600	0.43	15	2	7.5
Cd	114	28.7	8.99	220	680	0.32	15	10	1.5
In	115	95.7	5.79	1900	3300	0.58	6	2	3.0
Sb	121	57.4	8.64	340	480	0.71	30	8	3.8
Ba	138	71.7	5.79	2100	1300	1.6	3	4	0.75
La	139	99.9	5.58	2300	2300	1.0	10	4	2.5
Ce	140	88.5	5.47	2000	2300	0.87	6	2	3.0
Dy	164	28.2	5.93	520	850	0.61	40	8	5.0
Pb	208	52.4	7.42	430	1200	0.36	4	0.7	5.7
Bi	209	100	7.29	640	1900	0.34	20	2	10
Th	232	100	6.95	750	2600	0.29	20	4	5.0
U	238	99.3	6.1	760	2800	0.27	20	3	6.7

* ppt = parts per 10^{12}.

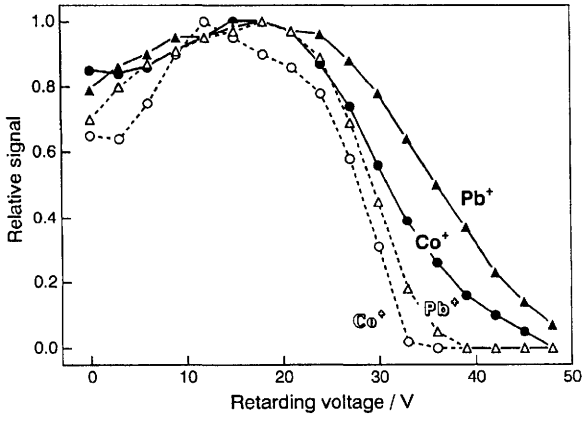

Fig. 6 Distributions of analyte ion kinetic energy in the N_2 and Ar ICPs: solid line, N_2 ICP; dashed line, Ar ICP

introduced water. The effect of the introduced water on monoxide ion formation should be observed more readily at lower sampling depths[18] and higher carrier gas flow rates. Further, a wide distribution of the kinetic energy might also affect oxide formation. A high concentration of ions with lower kinetic energy does not preclude monoxide formation.

Matrix Effects

Matrix effects on the analyte ion signals were investigated with co-existing Li (m/z = 9, IP = 5.39 eV) or Tl (m/z = 200, IP = 6.11 eV). The results obtained for Co^+ and Pb^+ as the analytes are shown in Fig. 7. As a 10 ppb solution of Co and Pb was

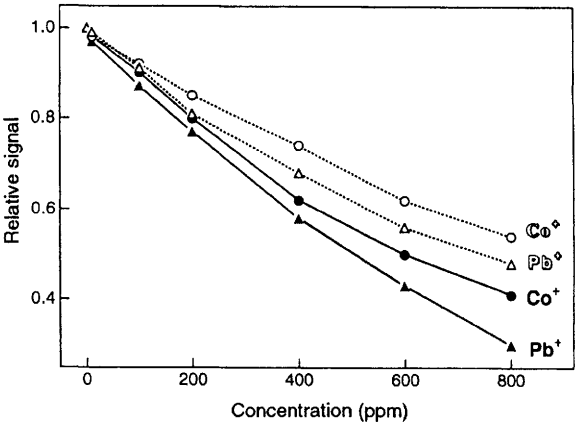

Fig. 7 Effects of the co-existing elements, Li and Tl, on the ion signals of Co^+ and Pb^+: solid line, Li matrix; dashed line, Tl matrix

Table 4 Signal ratios of doubly charged and monoxide ions to singly charged analyte ions

			N_2 ICP		Ar ICP	
Element	First IP/ eV	Second IP/ eV	$M^{2+}:M^+$	$MO^+:M^+$	$M^{2+}:M^+$	$MO^+:M^+$
Y	6.38	12.23	0.0019	0.035	0.046	0.020
Mo	7.10	16.15	0.073	0.053	0.0017	0.0027
Ba	5.21	10.00	0.0018	0.021	0.51	0.0095
Ce	5.47	10.85	0.0022	0.071	0.13	0.054
Pb	7.42	15.03	0.019	0.022	0.0017	0.00015

used, the matrix concentration was 1000–100 000 times that of the analyte. The analyte signal decreases with an increase in the matrix concentration. One of the common reasons for signal suppression in both ICPs is the decrease in sample introduction rate to the plasma, since the aspiration rate and nebulization efficiency decrease with an increase in the matrix concentration. As can be seen in Fig. 7, greater signal suppression was found with co-existing Li compared with Tl. In contrast, co-existing Tl suppressed the signals more than Li in both the 27.12 and 40.68 MHz Ar ICPs, where the same sample introduction device as employed in the present system was commonly used.[18]

Hence, two types of interference are presumed. The first is the disturbance of the ion beam path through the ion optics and mass spectrometer. This is known as the space charge effect, and is readily observed in the determination of light elements or in the presence of co-existing heavy elements.[24] However, the results obtained in this work cannot be adequately explained in terms of the space charge effect, because the light element Li causes greater suppression of the ion signals than the heavy element Tl. Another type of interference might be ionization interference by easily ionized elements. The ionization of Li, which is used as an ionization buffer in flame atomic absorption spectrometry, might disturb that of Co^+ and Pb^+. Ionization interference has been observed at higher carrier gas flow rates in Ar ICP-AES[25] and ICP atomic fluorescence spectrometry.[26] Ionization interference might be the reason for the signal suppression shown in Fig. 7, since a high flow rate of the N_2 central gas was adopted in order to achieve adequate sensitivity in the proposed N_2 ICP. In contrast, ionization interference makes a smaller contribution to the signal suppression at moderate central gas flow rates in Ar ICPs.[18]

REFERENCES

1 Date, A. R., and Gray, A. L., *Applications of Inductively Coupled Plasma Mass Spectrometry*, Blackie, Glasgow, 1989.
2 Tan, S. H., and Horlick, G., *Appl. Spectrosc.*, 1986, **40**, 445.
3 Evans, E. H., and Ebdon, L., *J. Anal. At. Spectrom.*, 1989, **4**, 299.
4 Evans, E. H., and Ebdon, L., *J. Anal. At. Spectrom.*, 1990, **5**, 425.
5 Lam, J. W., and McLaren, J. W., *J. Anal. At. Spectrom.*, 1990, **5**, 419.
6 Beauchemin, D., and Craig, J. M., *Spectrochim. Acta Part B*, 1991, **46**, 603.
7 Craig, J. M., and Beauchemin, D., *J. Anal. At. Spectrom.*, 1992, **7**, 937.
8 Lam, J. W. H., and Horlick, G., *Spectrochim. Acta, Part B*, 1990, **45**, 1327.
9 Lam, J. W., and Horlick, G., *Spectrochim. Acta, Part B*, 1990, **45**, 1313.
10 Hill, S. J., Ford, M. J., and Ebdon, L., *J. Anal. At. Spectrom.*, 1992, **7**, 719.
11 Wang, J., Evans, E. H., and Caruso, J. A., *J. Anal. At. Spectrom.*, 1992, **7**, 929.
12 Louie, H., and Soo, S. Y.-P., *J. Anal. At. Spectrom.*, 1992, **7**, 557.
13 Tanaka, T., Yonemura, K., Obara, K., and Kawaguchi, H., *Anal. Sci.*, 1993, **9**, 765.
14 Sheppard, B. S., and Caruso, J. A., *J. Anal. At. Spectrom.*, 1994, **9**, 145.
15 Montaser, A., and Golightly, D. W., *Inductively Coupled Plasmas in Analytical Atomic Spectrometry*, VCH, New York, 1987, p. 563.
16 Barnes, R. M., and Meyer, G. A., *Anal. Chem.*, 1980, **52**, 1525.
17 Yang, P., Barnes, R. M., Vechiarelli, J., and Uden, P. C., *Appl. Spectrosc.*, 1990, **44**, 531.
18 Uchida, H., and Ito, T., *J. Anal. At. Spectrom.*, 1994, **9**, 1001.
19 Gray, A. L., *J. Anal. At. Spectrom.*, 1986, **1**, 247.
20 Nonose, N. S., Matsuda, N., Fudakawa, N., and Kubota, M., *Spectrochim. Acta, Part B*, 1994, **49**, 955.
21 Oishi, K., Okumoto, T., Iino, T., Koga, M., Shirasaki, T., and Furuta, N., *Spectrochim. Acta, Part B*, 1994, **49**, 901.
22 Olivares, J. A., and Houk, R. S., *Appl. Spectrosc.*, 1985, **39**, 1070.
23 Gray, A. L., and Williams, J. G., *J. Anal. At. Spectrom.*, 1987, **2**, 599.
24 Tan, S. H., and Horlick, G., *J. Anal. At. Spectrom.*, 1987, **2**, 745.
25 Kalnicky, D. J., Fassel, V. A., and Kniseley, R. W., *Appl. Spectrosc.*, 1977, **31**, 137.
26 Kosinsky, M. A., Uchida, H., and Winefordner, J. D., *Anal. Chem.*, 1983, **55**, 688.

Paper 5/020851
Received April 3, 1995
Accepted July 17, 1995